Desalination and Water Treatment
www.deswater.com
doi: 10.5004/dwt.2023.29564

294 (2023) 185–201
May

Evaluation of modified bentonite using chemical and physical methods for removal of amoxicillin from aqueous solutions: batch and continuous study

Aseel Mohammed Naji, Ziad Tark Abd Ali*

Department of Environmental Engineering, College of Engineering, University of Baghdad, Baghdad, Iraq, emails: z.teach2000@yahoo.com (Z.T. Abd Ali) ORCID: https://orcid.org/0000-0001-9834-7122, aseel.najy2011m@coeng.uobaghdad.edu.iq (A.M. Naji)

Received 24 December 2022; Accepted 11 April 2023

ABSTRACT

The aim of this study is to modify the Iraqi natural bentonite (NB), as low-cost and available raw material, using different methods and investigate the potential application of using it as a reactive material for the removal of amoxicillin (AMX) from an aqueous solution in batch and continuous experiments. The modified bentonite (MB) was synthesized using different methods: (1) mixing NB with cationic surfactants (long and short alkyl chain surfactants symbolized as cetyltrimethylammonium bromide and tetramethylammonium bromide), respectively, and (2) thermal activation method to produce calcined bentonite. Surface area, scanning electron microscopy, and Fourier-transform infrared spectroscopy are used to describe the synthesized MB. Numerous elements that influence the amount of AMX removed, including contact duration, pH, the rate of agitation, initial concentration, and dose of the sorbent, have all been investigated. Two isotherm models (Langmuir and Freundlich), two kinetic models (pseudo-first-order and pseudo-second-order), and five breakthrough curve models were used to fit the column experimental data (Bohart–Adams model, Thomas–BDST model, Yan model, Belter–Cussler–Hu model, and Clark model). The outcomes of the experiments demonstrated that the modifications increased the effectiveness of NB's removal and this made it a reactive material that could be effective for removing AMX from aqueous solutions.

Keywords: Amoxicillin; Modified bentonite; Sorption; Isotherm; Kinetic

1. Introduction

Antibiotics have been used in human and veterinary medicine for several decades, but these compounds pose potential risks to aquatic and terrestrial organisms when released into the environment, for example in the aquatic environment, the emergence of antibiotic-resistant bacteria/resistance genes [1]. Amoxicillin (AMX) is a broad-spectrum penicillin antibiotic with two major components: an inner-lactam and a side chain known as dhidroxiphenilglicin. In veterinary pharmacies, it is commonly used to treat bacterial infections of the gastrointestinal and systemic systems. It is also commonly used to treat bacterial infections in human prescription drugs. Studies on the adsorption of the antibiotic amoxicillin onto bentonite and activated carbon have been conducted, and the findings show that amoxicillin's adsorption onto activated carbon is essential [2], however, costly activated carbons are the adsorbents used in this process the most frequently (GACs) [3]. In conventional sewage treatment facilities, a number of techniques have been tried to remove antibiotics, including biological processes, filtration, coagulation, flocculation, and sedimentation. However, new strategies are required as they have proven ineffective. For this purpose, the efficiency of the adsorption technique is demonstrated by the elimination of effluent pollutants at low concentrations (1 mg/L). While pharmaceutical

* Corresponding author.

component concentrations in raw home wastewater are often reported in the 100 ng/L – 10 g/L range, concentrations in hospital and pharmaceutical company effluents can vary from 100 to 500 mg/L. In comparison to other technologies, such as advanced oxidative processes, this method is simple to operate, low in cost, and does not introduce by-products into water [4,5]. As a result, there is a great deal of interest in developing low-cost alternative adsorbents.

In numerous studies, the capacity of bentonite to remove amoxicillin from aqueous solutions has been examined [6–8]. However, due to the hydrophilic nature of clay's mineral surface, amoxicillin adsorption capability was limited. Cationic surfactants are polar organic compounds with hydrophobic parts. The long alkyl chain is usually hydrophobic, it changes the hydrophilic nature of bentonite to hydrophobic when it interacts with bentonite layers. Since natural bentonite carries a negative charge on its surface, therefore, the bentonite surface charge is converted to a positive charge after modification. Numerous studies on the features of organoclays have been done as a consequence of their potential to function as good sorbents in removing organic pollutants from groundwater and wastewater [9].

There is much research dealing with the removal of amoxicillin (AMX) using modified bentonite, as mentioned above, most of them used batch mode only and avoided the continuous mode, due to the low hydraulic conductivity of natural and modified bentonite that considers a negative effect, especially on the continuous mode, as it clogs the bed and impedes water flow. In this work, the continuous mode was used in addition to the batch mode. The granules of glass waste were added to the modified bentonite to increase the hydraulic conductivity of the bed and reduce its clog.

The goal of this work was to remove amoxicillin from an aqueous solution using bentonite modified by two methods: The first one is mixing natural bentonite with cationic surfactants. Surfactants are intercalated inside the interlayer space by cation exchange [10]. A hydrophobic feature and an increase in interlayer space in the resulting modified bentonite make it suited for sorbing organic pollutants. Their density and the type of intercalated surfactants have the most effects on how efficiently they can adsorb substances.

Thermal activation is a further technique for changing bentonite. In the past, bentonite and clays that had been heated up were used to create bricks for construction and soil stabilization. The physico-chemical characteristics of bentonite, such as its water content, cohesiveness, and specific gravity, are changed by thermal treatment [11]. In addition, dehydration and dehydroxylation processes during bentonite thermal treatment could be attributed to octahedral cation movements inside the octahedral sheet. As a result, the adsorption capacity of bentonite is enhanced [12]. Finally, this study can be considered an attempt to evaluate the modification of natural bentonite using chemical and physical methods to improve it AMX removal efficiency, mechanical properties, and stability through batch and continuous modes.

2. Materials and methods

2.1. Materials

The native bentonite in its original state was the type of bentonite used in this research (calcium base). It was supplied by the State Company of Geological Survey and Mining (Baghdad) as pieces of rocks. These rocks were washed with distilled water several times, dried at 90°C, crushed into granules of different sizes, then sieved using sieves to produce bentonite granules of sizes 250–500 μm. The physical characteristics and composition of the natural bentonite (NB) were analyzed in the laboratories of the State Company of Geological Survey and Mining; the results are listed in Table 1. Two long and short alkyl chain surfactants were used, called cetyltrimethylammonium bromide (CTAB) and tetramethylammonium bromide (TMAB), respectively. In addition, amoxicillin was selected as a contaminant to simulate the water's amoxicillin contamination. It was obtained as trihydrate from the local market. Amoxicillin was dissolved in distilled water at a ratio of 0.05 g/L to produce a concentration of 50 mg/L, which was then used to create the aqueous solutions that resemble polluted water. All reagents of analytical grade were used without further purification. The initial pH of each of the solutions was adjusted by the addition of HCl or NaOH solution.

2.2. Synthesis of modified bentonite

The Iraqi natural bentonite (NB) was used in this study as a raw material to produce three types of modified bentonite (MB) using two cationic surfactants (CTAB and TMAB) and a thermal process to calcine the NB, these types of MB are symbolized by NB-CTAB, NB-TMAB, and calcined bentonite (CB), respectively. The first two types of MB (NB-CTAB and NB-TMAB) were prepared by adding 10 g of natural bentonite (NB) to 100 mL of distilled water. The mixture was mixed for 2 h, causing it to swell and become homogeneous. The desired amount of surfactant (CTAB or TMAB) was then added in weight ratios of 0.2, 0.25, 0.3, 0.35, 0,4, 0.45, 0.5, 0.55, 0.6 and 0.65 g surfactant/g NB mixture, then the mixing process is continued for 2 h. The resulting samples (mixtures), called modified bentonite (NB-CTAB and NB-TMAB), were

Table 1
Characteristics of natural Iraqi bentonite

Characteristics	Value
Physical	
Particle size, μm	250–500
Moisture content, %	6.57
Bulk density, kg/m^3	845
Specific surface area, m^2/g	63.5
Cation exchange capacity, meq/100 g	65
Composition (wt.%)	
Silica (SiO_2)	57
Aluminum (Al_2O_3)	13.5
Ferric oxide (Fe_2O_3)	4.5
Magnesium oxide (MgO)	2.35
Calcium oxide (CaO)	8
Sodium oxide (Na_2O)	0.7
Potassium oxide (K_2O)	0.4
Titanium oxide (TiO_2)	0.75
Loss on ignition (LOI)	12.8

washed several times with distilled water to remove excess salts and then dried in an oven at 90°C. The modified bentonite samples produced were ground and sieved to a size range of 250–500 μm. The CTAB or TMAB/NB weight ratio that achieves the maximum amoxicillin removal percent was adopted in the synthesis of the modified bentonite in all subsequent experiments (batch and continuous). Depending on the length of the alkyl chain, the two surfactants used in this study regulate the expansion of the interlayer space, for example the incorporation of the surfactants results in organoclays with a layer spacing restriction of 1.4–1.5 nm below a carbon number of 8 (case of TMAB) [9,13]. In contrast, depending on the concentration of a surfactant, CTAB with a long 16-carbon alkyl chain causes the creation of various configurations, including mono, lateral bilayer(s), and a paraffin structure (normal bilayer) inside the interlayer space [6,7]. Another approach was used in this study to produce the third type of MB (CB) through the thermal activation of bentonite to increase its mechanical resistance, dehydroxylation, eliminate some impurities, and improve the adsorption capacity [14,47]. Therefore, the natural bentonite was calcined for 24 h at 500°C to produce the calcined bentonite (CB).

2.3. Characterization of modified bentonite

The characteristics of NB and MB (NB-CTAB, NB-TMAB, and CB) have been studied through various analyzes as follows:

2.3.1. Fourier-transform infrared spectroscopy

Through the use of Fourier-transform infrared spectroscopy (FTIR) analysis, surface functional groups that are present on the sorbet may be identified, which also enables spectrophotometry observation [15]. Spectrum analysis in the 400–4,000 cm^{-1} range was performed with a Bruker Tensor 27 spectrophotometer (USA) using the KBR pellet technique. It is achieved at the College of Sciences of Tehran University.

2.3.2. Scanning electron microscopy

By using scanning electron microscopy (SEM) analysis (NOVASEM, FEL450L) at a voltage of 10 kV and a current of 6 mA, the morphology of the bentonite surface was evaluated. This flavor demonstrates how the structural characteristics of bentonite have changed both before and after treatment. It is earned at Tehran University's College of Science.

2.3.3. Surface area

When identifying the active sites that contaminants occupy, the surface area is a crucial consideration [16]. Using an ASTM D 3663, USA, micrometer to measure nitrogen adsorption at 77 K, a surface area analyzer and the Brunauer–Emmett–Teller technique were used to determine the specific surface area. It presented a performance at the Tehran University's College of Science.

2.4. Batch experiments

Under diverse settings, batch experiments were used to study the sorption of amoxicillin (AMX) by synthetically produced modified bentonite. A predetermined quantity of the MB was added to 100 mL of amoxicillin synthetic solution, which had a concentration of 50 mg/L, to conduct the batch removal studies. The mixture was then agitated using an orbital shaker (Edmund Buhler SM25, Germany). Batch studies with different contact times between 0 and 4 h, pH of solutions between 2 and 11, agitation rates between 0 and 250 rpm, initial amoxicillin concentrations between 50 and 250 mg/L, and sorbent doses between 0.05 and 1 g/100 mL were performed for practical purposes. In order to determine the quantity of amoxicillin that was still present in the solution, a predetermined volume of the solution was collected from each flask and filtered through filter paper of the type Whatman to separate the adsorbent from the aqueous solution. The filtered solution of amoxicillin (AMX) was then analyzed using a double-beam UV spectrophotometer at λ_{max} = 228 nm. All samples were re-examined three times to ensure the accuracy of the results. The amount of amoxicillin adsorbed onto the modified bentonite, q_e, was calculated using the following equation [17,18]:

$$q_e = \frac{\left(C_0 - C_e\right)V}{m} \tag{1}$$

where q_e (mg/g) is the amount of drug adsorbed per unit mass of adsorbent, C_o and C_e (mg/L) are the initial and equilibrium concentrations of drug, respectively. V (L) is the volume of drug solution and m (g) is the adsorbent mass. Eq. (2) was used to calculate the removal % (R%) of AMX from MB [19,20]:

$$R = \frac{\left(C_0 - C_e\right)}{C_0} \times 100\% \tag{2}$$

2.5. Isotherm models

Two isothermal models were utilized to characterize the sorption data, as can be seen in the next sections [21,22]:

2.5.1. Langmuir model

The Langmuir isotherm model is given through the formulation of a monolayer, uniform, and finite adsorption site, which ends up in a saturation value wherein no greater adsorption takes place beyond. It additionally assumes that molecules adsorbed on neighboring sites do not interact with one another as in Eq. (3).

$$q_e = \frac{q_m b C_e}{1 + bC_e} \tag{3}$$

where b is the constant of the free energy of sorption (L/mg), and q_m is the maximum sorption capacity (mg/g), and C_e (mg/L) is the equilibrium concentration of the contaminant in the bulk solution. The linearized form of the Langmuir model could be written as in Eq. (4):

$$\frac{C_e}{q_e} = \frac{1}{q_m b} + \frac{1}{q_m} C_e \tag{4}$$

The Langmuir constants, q_m and b, are determined from the slope and intercept of the C_e/q_e against C_e plot, respectively.

2.5.2. Freundlich model

Adsorption processes on heterogeneous surfaces can be described by the Freundlich isotherm. This isotherm defines the heterogeneity of the surface and the exponential distribution of the active sites and their energy. This equation may be used to represent this model:

$$q_e = K_F C_e^{1/n} \tag{5}$$

where K_F is the intensity of sorption is indicated by the Freundlich sorption coefficient, where n is an empirical coefficient, is (mg/g)(L/mg)$^{1/n}$. The above equation could be described with linearized form as in Eq. (6):

$$\ln q_e = \ln K_F + \left(\frac{1}{n}\right)\ln C_e \tag{6}$$

The values of K_F and n can be calculated by plotting of $\ln q_e$ vs. $\ln C_e$, which they correspond to the intercept and slope of the plot, respectively.

2.6. Kinetics study

To comprehend the workings of the drug sorption technique (AMX) in modified bentonite, kinetic sorption models were applied. Pseudo-first-order and pseudo-second-order are two of these models [23]:

2.6.1. Model of pseudo-first-order

The following equation can be used to compute the sorption rate over time [20]:

$$\frac{dq_t}{dt} = k_1\left(q_e - q_t\right) \tag{7}$$

where q_e represents the amount of contamination sorbed at equilibrium (in mg/g), k_1 represents the pseudo-first-order adsorption rate constant in (min^{-1}), and q_t represents the amount of contamination sorbed at time t (in mg/g). The linear version of Eq. (7) becomes: after integration and the application of boundary conditions, $t = 0$ to t and $q_t = 0$ to q_e [24]:

$$\ln\left(q_e - q_t\right) = \ln\left(q_e\right) + k_1 t \tag{8}$$

The values of q_e and k_1 can be obtained from the slope and intercept of the plot $\ln(q_e - q_t)$ vs. t, respectively.

2.6.2. Model of pseudo-second-order

The contaminated monolayer must be attached to the sorbent surface, the sorbent must have an equal sorption energy, and there must not be any interaction between the sorbed contaminants. These assumptions may be phrased as follows in Eq. (9) [25]:

$$\frac{dq_t}{dt} = k_2\left(q_e - q_t\right)^2 \tag{9}$$

For the same boundary conditions, the linear form becomes as in Eq. (10) [26]:

$$\frac{t}{q_t} = \frac{1}{k_2 q_e} + \frac{t}{q_e} \tag{10}$$

where k_2 is the pseudo-second-order rate constant (g/mg·min). The values of q_e and k_2 can be obtained from the slope and intercept of the plot t/q_t vs. t, respectively.

2.7. Experimenting with column

Using the efficiency of contaminant removal and the coefficient of hydraulic conductivity as indicators, the column experiments for the removal of AMX from contaminated water were put to the test to investigate the reactivity and hydraulic behavior of filler materials [27]. The column structure used in this inquiry is presented in Fig. 1. The following sample ports were installed at intervals of 5 cm (P1), 10 cm (P2), 15 cm (P3), 20 cm (P4), and 25 cm (P5) from the bottom of the column, which was made of an acrylic cylinder with a diameter and height of 2 and 50 cm, respectively. Plastic valves are used to create these shaft length openings. As schematically depicted in, the sorbent was added to the column (Fig. 1). Using a peristaltic pump, distilled water was gradually introduced into the material from the bottom of the column while being forced upward through the sorbent material until it became gradually saturated. Due to the upward movement that drives the air in front of it, air entrapment between the sorbent material's particle particles won't occur. The column tests were conducted at room temperature, and over the course of a 160-h period, several measurements of the AMX concentration in the effluent water were made. Immediately after that, water samples were placed into test tubes and examined using a UV spectrophotometer. All samples were re-examined three times to ensure the accuracy of the results. The constant-head permeability approach was used to determine the hydraulic conductivity (K) as a function of time in Eq. (11):

$$k = \frac{Q / A}{\Delta h / \Delta l} \tag{11}$$

where Q is the solution flow rate, Δh is the hydraulic head drop, Δl is the length of the sorbent pattern, and A is the cross-sectional area of the column [28].

2.8. Contaminant transport in porous media and breakthrough curves models

Mathematically, the transport of the pollutants across porous media may be described by the advection–dispersion equation (Eq. 12). According to this equation, advection, dispersion, and sorption are the three processes that control the movement of dissolved contaminants. Advection is the migration of the pollutant with flowing water, while dispersion is the migration of the pollutant due to the concentration gradient and different pathways [29,30].

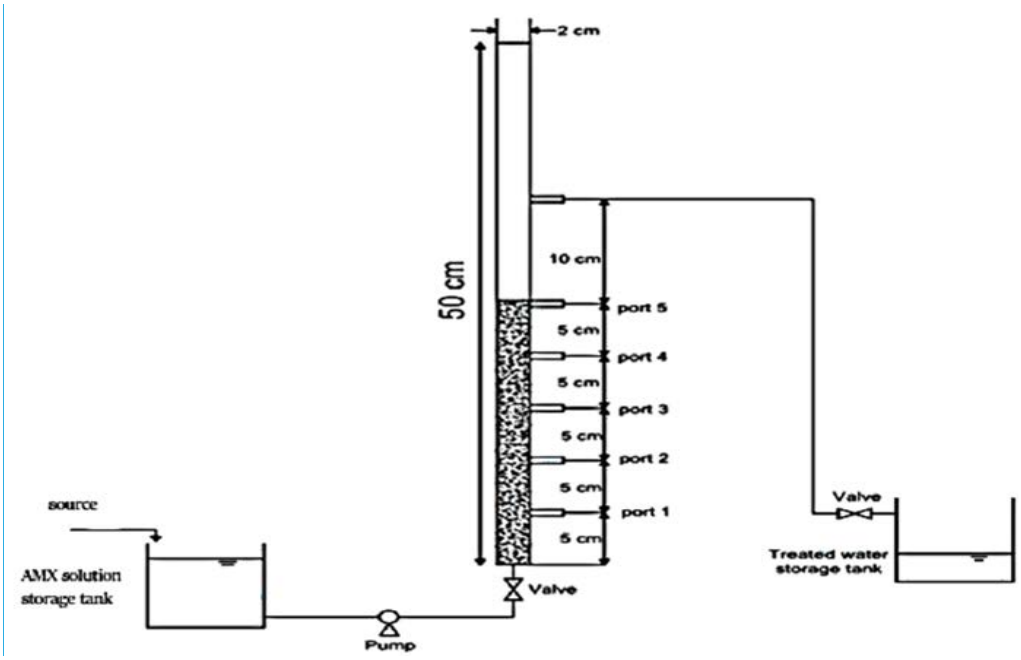

Fig. 1. Schematic diagram of laboratory-scale column.

$$\frac{\partial C}{\partial t} = \left(\frac{D_z}{R}\right)\frac{\partial^2 C}{\partial z^2} - \left(\frac{V_z}{R}\right)\frac{\partial C}{\partial z} \tag{12}$$

$$R = 1 + \frac{\rho_b}{n}\frac{\partial q}{\partial C} \tag{13}$$

It may be expressed using the equation below, where V_z is the pore water velocity (mm/s), D_z is the hydrodynamic dispersion coefficient (m^2/s), and R is the factor of retardation [4].

where n is the porosity of the porous media, q is the quantity of contaminant that has been sorbed onto the sorbent material (mg/g), and ρ_b is the bulk density (kg/m^3). Eq. (12) may be solved using both numerical and analytical methods, and the results of the analysis can be given in terms of time and location together with the values of C for the flow domain. It is possible to identify the S-shaped breakthrough curve by plotting the concentration vs time at a specific location in the flow scope [23,31]. Empirical models, which are easier to use and maintain and avoid the numerical solution, were utilized in the current work to simulate the breakthrough curves in the packed column. Following is a quick summary of these models [32,33]:

2.8.1. Bohart–Adams model (1920)

The model Bohart–Adams makes the assumption that the sorption rate is proportional to the adsorbent's residual capacity as well as its species concentration. The shape of this model is as follows:

$$\frac{C}{C_0} = \frac{1}{1 + \exp\left(KN_0\frac{Z}{U} - KC_0 t\right)} \tag{14}$$

where C_o and C represent the initial and instantaneous concentrations of the pollutant in the solution (mg/L), K represents the kinetic constant (L/g·min), N_0 represents the saturation concentration (mg/L), Z represents the bed depth in the column (cm), t represents the operation time (min), and U represents the flow rate (cm/min) [34].

2.8.2. Thomas–BDST model (1944)

It is a widely used model to explain the movement of non-conservative contaminants in packed columns, and its equation is shown below [35].

$$\frac{C}{C_0} = \frac{1}{1 + \exp\left[\frac{K_T}{Q}qM - K_T C_0 t\right]} \tag{15}$$

where C_o and C are the influent and effluent concentrations, respectively (mg/L), K_T is the Thomas rate constant (mL/mg·min), q is the maximum adsorption capacity (mg/g), M is the amount of adsorbent in of the column (g), t is the adsorption time (min) and Q is the feed flow (mL/min).

2.8.3. Yan model (2001)

The Yan model, or what many publications call the dose-response model, is represented as follows [36]:

$$\frac{C}{C_0} = 1 - \frac{1}{1 + \left(\left(\frac{0.001 \times Q \times C}{q_0 \cdot M}\right) \times t\right)^a} \tag{16}$$

where q_0 is the maximum capacity for sorption (mg/g), and a is a constant with respect to the model's slope.

Estimating the constants in this model can be done using nonlinear regression with measurements from continuous experiments.

2.8.4. Clark model (1987)

Clark assumed that pollutant adsorption obeys the Freundlich model and the following kinetic formula was developed [37].

$$\left(\frac{C}{C_0}\right)^{n-1} = \frac{1}{1 + A \cdot e^{-rt}} \tag{17}$$

where n is the exponent of the Freundlich isotherm, A and r are components of the kinetic equation.

2.8.5. Belter–Cussler–Hu model (1988)

Chu [38] suggested an enhanced semi-empirical fixed bed known as the Belter–Cussler–Hu model of the breakthrough curves of a symmetric form, which is denoted by the following equation [23]:

$$\frac{C}{C_0} = 1 + \text{erf}\left[\frac{\left(t - t_0\right)\exp\left(-\sigma\left(\frac{t}{t_0}\right)\right)}{\sqrt{2}\sigma t_0}\right] \tag{18}$$

where erf[x] is the error function of x, t is the column residence time, t_0 is the time at which the effluent concentration is half that of the influent concentration, and σ standard deviation, which is a measurement of the breakthrough curve slope in its straight component.

3. Results and discussion

3.1. Modification of natural bentonite

Different samples of modified bentonite (MB) were prepared and tested by mixing various amounts of surfactants (CTAB and TMAB) with a specified amount of natural bentonite at room temperature under specified conditions (time = 4 h, pH = 7, agitation speed = 200 rpm, C_o = 50 mg/L, and dosage = 0.5 g/100 mL), as shown in Fig. 2. It was observed that as the weight ratios (CTAB or TMAB/NB) increases, the AMX removal percentage increases until it reached the highest value of 79% and 48% at 0.5 g·CTAB/g·NB and 0.6 g·TMAB/g·NB, respectively, then the removal % starts to decrease as the ratios of (CTAB or TMAB/NB) increases to reach 75% and 45%, respectively. This behavior can be explained as follows: It is known that the surface of the bentonite has a negative charge, and when it is modified using cationic surfactants, its surface will acquire a positive charge, and thus the negatively charged particles of AMX will be attracted to it leading to an increase in the AMX removal percent. When adding more quantities of surfactant, which are more than the bentonite can accommodate, they will stay in the bulk solution and convert to a source to attract a part of the negatively charged ions of AMX and prevent them to reach the surface of modified bentonite, so, this part of AMX particles stay in the solution without removal, causing a decrease in the AMX removal percent [39]. Therefore, the ratios of (CTAB/NB = 0.5) and (TMAB/NB = 0.6) that achieved the higher removal percent were adopted in preparing the modified bentonite (NB-CTAB and NB-TMAB) which were used in all batch and continuous experiments in this study.

For the case of the production of calcined bentonite (CB), firstly, the NB was heated (80°C–105°C). The heating of NB to this temperature range leads to the loss of water, volatile compounds, microorganisms, and organic matter. The loss of these elements does not change the structure of the clay. After that, the temperature range was increased to 450°C–500°C, which led to the loss of hydroxyl that begins to change the structure of the bentonite. The hydroxyl loss is interesting for the process, it increases the stability of the clay for its use in the fixed-bed adsorption column [11].

In order to clarify the effectiveness of bentonite modification processes and their impact on increasing the bentonite activity, the CB and NB were tested to use in removing AMX from aqueous solutions under the same conditions that are illustrated in Fig. 2. The result of this test is presented in Table 2. It can be seen that the AMX removal percent was increased by 6.58, 4 times, and 6 times using NB-CTAB, NB-TMAB, and CB in comparison to using NB. This was caused by the bentonite layer's alteration, which raised the layer's spacing and changed the hydrophilic surface of the material into one that was hydrophobic to boost its adsorptive capabilities [40].

3.2. Characterization of reactive materials

3.2.1. Fourier-transform infrared spectroscopy

By using FTIR analysis, it is feasible to identify the surface functional groups that are present on the adsorbent,

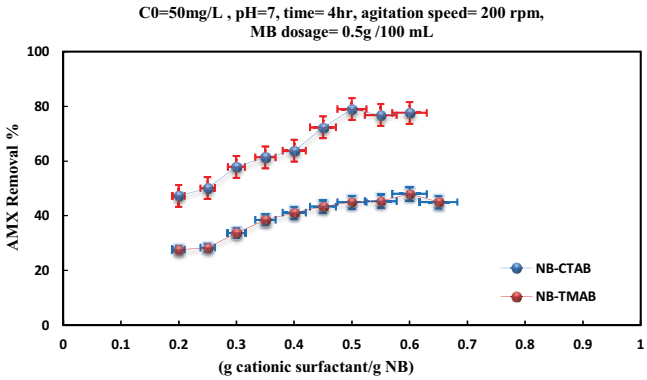

Fig. 2. Effect of the ratio of CTAB or TMAB/NB for the removal of amoxicillin.

Table 2
Comparison of amoxicillin removal by natural and modified bentonite

Contaminant	NB	NB-CTAB	NB-TMAB	CB
Amoxicillin	12%	79%	48%	72%

which also allows for spectrophotometric observation. These spectrums were measured between 400–4,000 cm^{-1}, as shown in Fig. 3. This procedure was carried out for NB, NB-CTAB, NB-TMAB, and CB. The large absorption bands that are seen at 3,799; 3,626 and 3,400 cm^{-1} on natural bentonite are due to the O–H stretching vibrations of the Si–OH (silanol) and Al–OH groups, respectively also strong band at 1,028 and 470 cm^{-1} represents the Si–O–Si groups of the tetrahedral sheets.

After the modification of NB with CTAB, an asymmetric stretching mode of Si–O–Si has shifted from 1,028 to 1,037 cm^{-1}, also the deformation and bending mode of Si–O–Si at 470 cm^{-1} have shifted to 426 cm^{-1}. The additional peak at 1,473 cm^{-1} in NB-CTAB, which is absent in NB, indicate the presence of C–N vibration in tertiary amines. After being modified with CTAB, the absorption band of –OH and the bending vibration of H_2O of NB significantly shifted from a high frequency of 1,650 cm^{-1} to a low frequency of 1,637 cm^{-1}, indicating the removal of water molecules and a change in the hydrophobicity of natural bentonite. Peaks at 2,856 and 2,929 cm^{-1}, which are sharper than those of the NB and correspond to the symmetrical CH_3 stretching absorption band and the CH_2 scissor vibration band, respectively, were identified as the organic matter in NB-CTAB. The groups CH_3 and CH_2 demonstrate how the CTAB molecules were incorporated into the bentonite mineral layers. The FTIR measurements indicate that CTAB was used to modify the surface of the bentonite clay.

Asymmetry in the Si–O–Si stretching mode has changed from 1,028 to 1,045 after TMAB was used to modify natural bentonite. The deformation and bending mode of Si–O–Si has also changed from 470 to 451 cm^{-1}. The additional peaks at 1,423 cm^{-1} in NB-TMAB, which are absent in NB, indicate the presence of C–N vibration in TMAB.

When compared to the MB with CTAB, the organic matter in modified bentonite with TMAB had peak at 2,939 cm^{-1} that is less severe. These peaks were attributed to the symmetrical CH_3 stretching absorption band and the CH_2 scissor vibration band, respectively. The groups CH_3 and CH_2 showing that the use of TMAB to modify the surface of bentonite clay was successfully performed, according to FTIR data, which clearly shows that the molecules were intercalated between the layers of bentonite minerals.

The NB and calcined bentonite were also characterized using FTIR spectroscopy as illustrated in Fig. 3. The FTIR spectra of the natural bentonite and calcined bentonite were not much different. Fig. 3 shows that after thermal activation, the band of O–H stretching was reduced. This phenomenon indicates that the water content in interlayer of the thermal activated bentonite was reduced.

Comparing the FTIR spectra of modified bentonite before and after the sorption of amoxicillin revealed that the peak at 1,467 cm^{-1} indicated the existence of –C–N stretching vibration peak and tertiary amine in amoxicillin, whereas the peak at 2,850 cm^{-1} showed C–H groups. The shift in peak to 3,630 cm^{-1} demonstrates that (NB-TMAB, NB-CTAB, and CB) each have amoxicillin adsorb to the silanol group in a different way.

3.2.2. Scanning electron microscopy

SEM examination was used to illustrate the surface morphology and microstructure of NB before and after treatment as shown in Fig. 4. The surface morphology of the NB following the modification procedure underwent substantial modifications, as seen in this image. It is evident that NB has a porous structure, a rough and uneven look, and a dispersed block structure with various block sizes, while the surface morphology of NB-CTAB and NB-TMAB was smooth and accompanied by a few holes. This fluffy appearance probably occurs due to the reduction in certain amorphous phases originally associated with the bentonite because the surfactants (CTAB and TMAB) have generally covered the surface of the NB. The SEM image of the CB indicates that the thermal modification of NB can make it a more porous structure compared to raw bentonite due to the interlayer spaces having collapsed, resulting in a more tightly bound structure.

3.2.3. Surface area

The specific surface area is a crucial indicator of the adsorption capacity for adsorbents. The results of this test revealed that the MB using surfactants had a smaller surface area than NB. The surface area of NB was 46.22 m^2/g, this value reduced to 23.34 and 5.17 m^2/g for MB (NB-CTAB

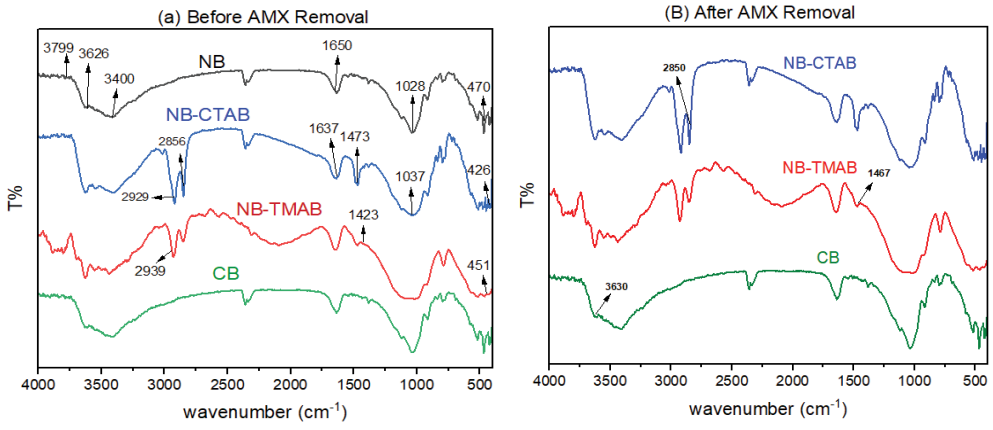

Fig. 3. Fourier-transform infrared spectra of NB and MB.

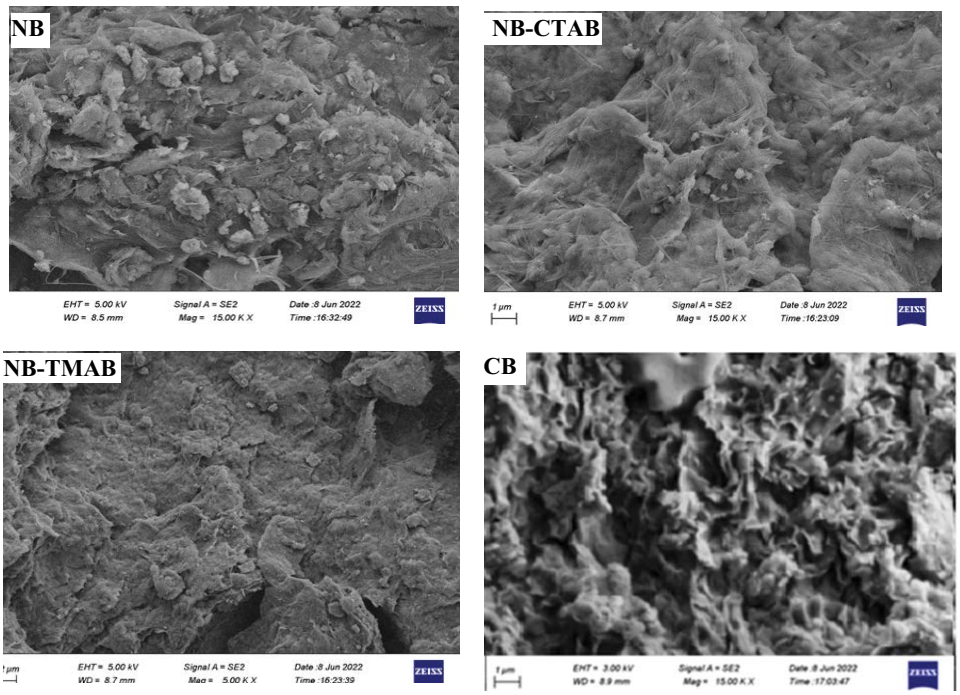

Fig. 4. Scanning electron microscopy images of NB and MB.

and NB-TMAB, respectively). This result can be attributed to the agglomeration property of NB after modification by surfactant. In addition, the organic molecules of surfactant entered into the interlayers of NB and overlapped its surface, which blocked the channel between the layers and reduced the surface area and pore volume. This result was similar to the research findings of many researchers [12,20].

In the case of CB, the obtained results showed that the thermal activation of NB improved the surface properties of raw bentonite. The surface area of CB was 72.37 m^2/g, which was larger than that of NB, because of the heat process used to remove the water molecules and volatile chemical compounds that adhere to the bentonite surface, CB has a greater surface area than raw bentonite, which is indicative of a more porous structure.

3.3. Influence of operational conditions in batch mode

3.3.1. Contact time

The amount of AMX removed by MB using surfactants and the thermal process was studied at different contact times with conditions illustrated in Fig. 5. This graph shows that as the contact duration rose, the amount of AMX that was removed increased as well. In addition, the sorption rate was high during the primary stage but gradually decreased after that. It is likely that the fewer MB active sites contributed to the slower sorption. The result shows that at a time (3.5 h) the maximum AMX removal percent of 79%, 48%, and 70% was achieved for NB-CTAB, NB-TMAB, and CB, respectively. It can be noted that the AMX removal percent for NB-CTAB was higher than NB-TMAB and CB. This result can be attributed to the fact that the adsorption of AMX depended not only on the partition mechanism, but also on the number of hydrocarbon chains within the surfactant

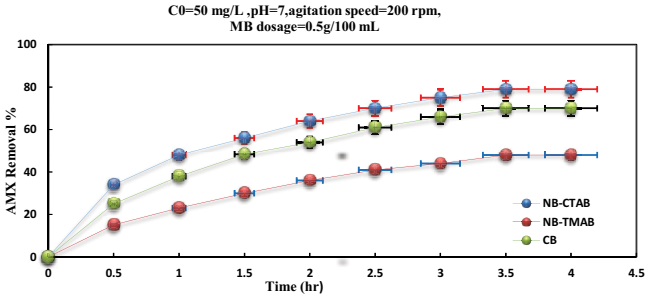

Fig. 5. Effect of contact time on the amoxicillin removal percent.

molecule that interlayered with NB [6,7]. The AMX removal percent for NB-CTAB was higher than NB-TMAB due to the NB-CTAB was treated with a longer chain surfactant (CTAB) which can bond with more AMX particles than another surfactant (TMAB), also, the NB-CTAB has a surface area higher than NB-TMAB according to the surface area test that illustrated the surface areas were 23.34 and 5.17 m^2/g for NB-CTAB and NB-TMAB, respectively. In addition, it is important to note that although the CB has a higher surface area than NB-CTAB, it has AMX removal percent lower than NB-CTAB. This behavior can be explained that the NB-CTAB has functional groups due to the presence of CTAB-surfactant that do not present in CB, which led to an increase in the affinity between AMX and NB-CTAB more than CB.

3.3.2. pH of solution

One of the most crucial elements impacting the adsorption capacity may be thought of as the initial pH of the AMX solution. This is because it has an impact on both the amount of the sorbate ionization and the surface charge of

the sorbent. Therefore, the sorption of AMX utilizing MB was investigated at various pH range between 2 and 11, as shown in Fig. 6.

As can be observed, the removal percentage of AMX employing cationic surfactants rose as the pH value climbed up to pH = 10, which produced the maximum removal percentages of 86% and 54% for NB-CTAB and NB-TMAB, respectively. After that, the removal percentage seems to have steadied somewhat. The following is an explanation for this behavior: at low pH values, there is an excess of H^+ protons on the active sites of the adsorbent, which compete with the cationic groups of the adsorbate, causing a lower adsorption rate of organic compounds, while when the pH values increases, the surface charge density of H^+ decreased, reducing the electrostatic repulsion between the positively charged adsorbent surface and the organic adsorbate, thereby increasing the extent of sorption process [42].

The results show that in the case of CB, the AMX removal percent increased as the pH value increased until it reached the highest removal % (82%) at a pH of 6, then the removal percent declined to reach the minimum removal % (17%) at a pH = 11. The CB is composed mostly of montmorillonite with a negative surface charge, while the AMX is a zwitterionic compound (pka_1 = 6.71 and pka_2 = 9.41), at pH lower than 6.71 (acidic conditions) AMX has a positive charge and pH higher than 9.41 (basic conditions) has a negative charge; Therefore, under conditions of this section, with increasing pH values up to 6, the positive charge of the AMX increased leading to the increase in the electrostatic attraction with the negative charge on the surface of CB causing to increase in the AMX removal percent. After that, the increase in pH values leads to an increase in the negative charge of AMX causing the increase in the electrostatic repulsion with a CB surface due to it containing a negative charge causing reduce the AMX removal percent. This explains the behavior of the CB with different pH values.

3.3.3. Agitation speed

By varying the agitation speed from 0 to 250 rpm while maintaining the other parameters constant, it was possible to determine how much the agitation speed affects the AMX elimination percentage. Fig. 7 shows that about 20%, 8%, and 14% of AMX were removed before vibration with NB-CTAB, NB-TMAB and CB, respectively, in addition, the percentage of AMX removal rises with increasing vibration rate until it reaches a higher value of 88%, 57% and 85% for NB-CTAB, NB-TMAB and CB, respectively. These results are explained by the fact that speeding up the agitation increases the amount of contaminant that diffuse to the surface of the reactive medium. A proper contact must be made between the sorbate in the solution and the binding sites in order to successfully transfer the sorbate to the sorbent sites [42].

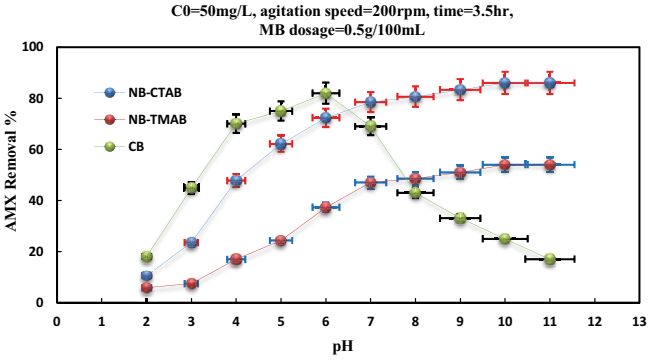

Fig. 6. Effect of solution pH on the amoxicillin removal percent.

3.3.4. Initial concentration

The impact of concentration values of AMX on the removal's ratio in the range of 50–250 mg/L was the examined in this series of tests. In fact, Fig. 8 clearly demonstrates the dramatic decrease in AMX removal percentage that occurred when the initial concentration was increased from 50 to 250 mg/L. The main reason for this drop in removal rates was due to the saturation of the adsorbent (MB) sites with AMX molecules.

3.3.5. MB dosage

The importance of the AMX removal using different MB dosages (0.05–1 g/100 mL) was investigated, as seen in Fig. 9. These results demonstrate that only 88%, 83%, and 56% of AMX were eliminated at 0.5 g of NB-CTAB, CB, and NB-TMAB, respectively, when added 100 mL of AMX solution. A considerable improvement in the elimination rate to 97%, 94%, and 68% for NB-CTAB, CB, and NB-TMAB, respectively, may be induced by increasing the MB dose to 0.8 and 0.9 g/100 mL for (NB-CTAB and CB) and (NB-TMAB), respectively. The reason for this behavior is that as sorbent

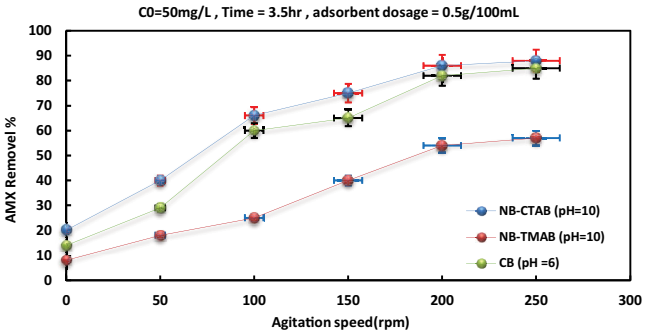

Fig. 7. Effect of agitation speed on amoxicillin removal percent.

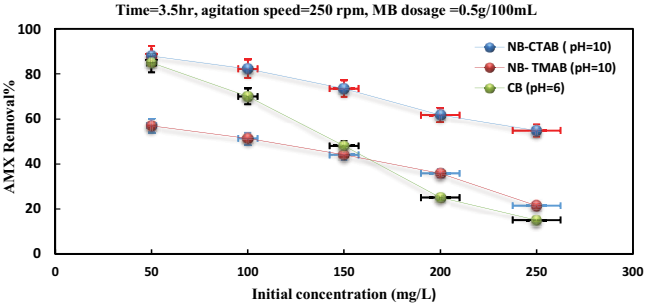

Fig. 8. Effect of initial concentration on the amoxicillin removal percent.

(MB) dosage is increased, the amount of open sites that are accessible to bind additional AMX molecules, surface area, and pore volume all increase. As a result, an increase in MB dosage results in an increase in removal percent. Additionally, it should be highlighted that the stability of the contaminant concentration that remains in the aqueous phase prevents an increase in dosage that exceeds 0.8 and 0.9 g/100 mL for (NB-CTAB and CB) and (NB-TMAB), respectively, from having a substantial impact on the AMX removal %. Table 3 summarizes the previous works that utilize modified bentonite for the removal of several organic contaminants from contaminated water.

3.4. Sorption isotherms

Two isotherm models, Langmuir and Freundlich, were used to match the experimental data from the sorption process. In light of this, Microsoft Excel 2016 was used to determine the slope and intercept of the linear plot in order to get the empirical coefficients for each model, as shown in Fig. 10. The determination coefficients and values of the isotherm model constants are listed in Table 4. In contrast to the Langmuir model, the Freundlich model clearly produced a larger value for the coefficient of determination (R^2), for the depiction of the sorption data of AMX, the Freundlich model is therefore more suited [43].

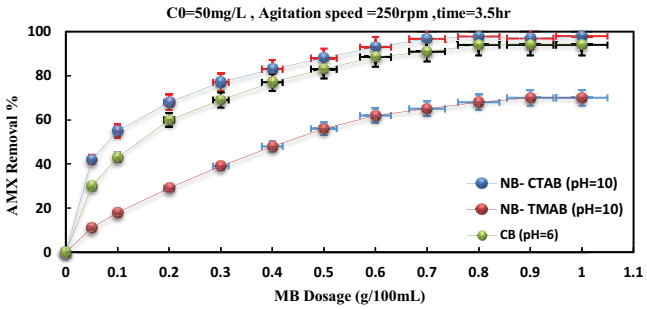

Fig. 9. Effect of adsorbent dosage on the amoxicillin removal percent.

3.5. Sorption kinetics

The kinetics data was correlated using the pseudo-first-order and pseudo-second-order models. Plotting of $\ln(q_e - q_t)$ and t/q_t vs. t for the linear plot of the first and pseudo-second-order models, as shown in Fig. 11. Using the Microsoft Excel 2016 program, based on the slop and the y-axis intercept of the straight line, the constants for these models were calculated. The values of the kinetic model constants and the coefficients of determination are reported in Table 5. Regardless of the amount of R^2, it is obvious that the uptake of AMX utilizing MB is most likely second-order since the (experimental) value of q_e was more similar to the (computed) q_e of the second-order model than the first-order model. These results show that chemoprevention was prevalent, and this result is consistent with the findings of other researchers such as [2,42,49].

3.6. Column experimentation

A clear acrylic column with five sampling ports was used to carry out a number of column experiments. as shown schematically in Fig. 1. In order to get the maximum AMX elimination percentage as shown in the batch trials, these studies were carried out with AMX solution under the optimal circumstances. Meanwhile, the following indications cast doubt on the column experiment results.

3.6.1. Measuring the initial value of hydraulic conductivity of MB

It is important to note that bentonite generally has a lower hydraulic conductivity than most common reactive media [41]. This property has a particularly negative effect on column experiments, as it clogs the bed and impedes water flow. To increase the hydraulic conductivity value and avoid bed blockages, broken glass waste (GW) was used in the current work. It is readily available and inexpensive material. The prepared MB (NB-CTAB, NB-TMAB, and CB) was mixed with the glass waste as an inert filler component before being used in the column experiments. The glass

Table 3
Summary of previous works

Adsorbent material	Type of modification	Contaminant	Adsorption capacity (mg/g) or removal %	References
Bentonite	Acid activation	Acid yellow Acid blue Acid red	Acid yellow = 71.1% Acid blue = 98.4% Acid red = 85.25%	[50]
Bentonite	Hexadecyl trimethyl ammonium bromide, HDTMA	Amoxicillin	81.9% at (C_o = 19 mg/L) 87.5% at (C_o = 2 mg/L)	[51]
Bentonite	Hexadecyl trimethyl ammonium bromide, HDTMA	Diclofenac sodium	388 mg/g	[52]
Bentonite	L-Tryptophan and $FeCl_2{\cdot}4H_2O$	Synthetic estrogen	4.20 mg/g	[53]
Bentonite	Cationic surfactants (CTAB & TMAB) and thermal activation	Amoxicillin	NB-CTAB = 96% NB-TMAB = 70% CB = 94%	Present work

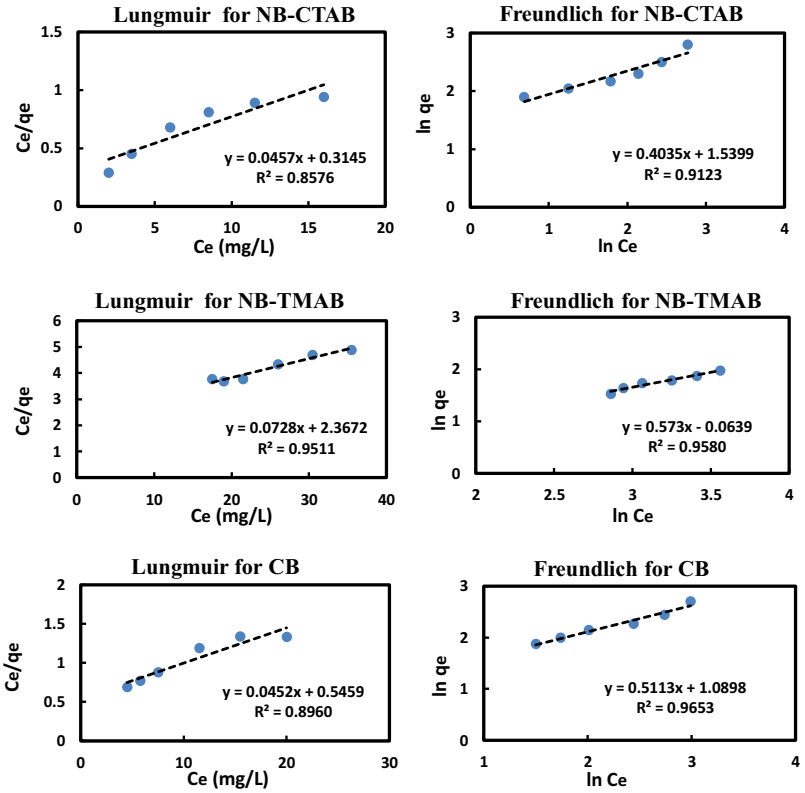

Fig. 10. Linear form of isotherm models for sorption of amoxicillin onto MB.

Table 4
Adsorption isotherm constants with determination coefficients for amoxicillin using MB

Model	Parameter	NB-CTAB	NB-TMAB	CB
Langmuir	q_m (mg/g)	21.8818	13.7362	22.1238
	b (L/mg)	0.1453	0.0307	0.0827
	R^2	0.8576	0.9511	0.8960
Freundlich	K_F (mg/g)(L/mg)	4.6641	0.9380	2.9736
	n	2.4783	1.7452	1.9557
	R^2	0.9123	0.9580	0.9653

waste was then washed, ground, and sieved at 250–500 nm. However, three tested reactive systems or mixtures (MB/GW) have been used in the column experiments by mixing the MB with GW. These systems were: M1 (2MB/1GW), M2 (2MB/2GW), and M3 (2MB/3GW). The hydraulic conductivity of these systems was determined at the Civil Engineering Department, University of Baghdad, as illustrated in Table 6. From the finding, the reactive system M2 (2MB/2GW) was found more appropriate than M1 (2MB/1GW) and M3 (2MB/3GW) because it maintains appropriate flow using the minimum quantity added of GW so that any decrease in the amount of the effluent water can be avoided for the preservation of the bed activity and maintenance of the acceptable hydraulic conductivity. It is worth noting that adding more quantity of GW, as in the M3 reactive system, will increase the hydraulic conductivity of the bed, as shown in Table 6, which means an increase in the flow, but at the same time, the quantity of the inert material (GW) increased too at the expense of the active material (MB) which leads to reduce the AMX removal efficiency, therefore the M3 reactive system was not suitable, also the M1 reactive system also not suitable because it has relatively low hydraulic conductivity that does not allow water to flow freely without clogging. The presence of GW facilitated the creation of large-sized voids that can interact with one another, removing any obstruction in the flow channel; Therefore, the reactive system of M2 (2MB/2GW) was adopted in all column experiments. It is important to note that tests have been done on the activity of glass granules (alone) in the removal of AMX and have shown that this material is inert because there is no discernible effect.

3.6.2. Monitoring the AMX concentrations in the effluent

One of the factors that must be considered to evaluate the performance of the reactive medium in removing AMX using a packed bed column is to determine the concentrations of contaminant in the effluent [44,47]. The normalized concentration (C/C_o) of AMX was measured in the effluent of the five ports during fixed time periods with an initial concentration of 50 mg/L and a flow rate of 5 mL/min as shown in Fig. 12. This figure showed that the AMX plume is restricted by the reactive media (MB/GW). Therefore, it plays an important role in limiting AMX dispersal in the column and can be successfully used as a reactive material to remove AMX. However, as the operation time increases,

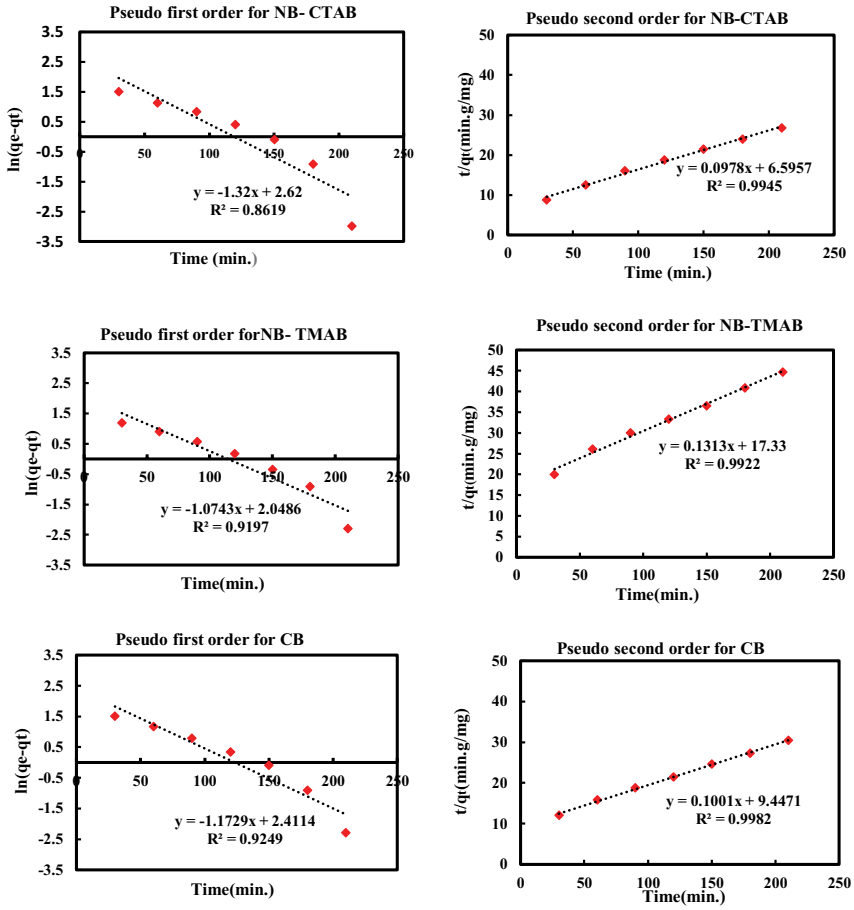

Fig. 11. Kinetic models for the sorption of amoxicillin onto MB.

Table 5
Kinetic models parameters with determination coefficients

Model	Parameter	NB-CTAB	NB-TMAB	CB
Pseudo-first-order	k_1 (min^{-1})	1.3200	1.0743	1.1729
	q_e (experimental, (mg/g))	7.9000	4.8000	7.0000
	q_e (calculated, (mg/g))	13.7300	7.7500	11.1400
	R^2	0.8619	0.9197	0.9249
Pseudo-second-order	k_2 (mg/g·min)	0.0014	0.0009	0.0010
	q_e (experimental, (mg/g))	7.9000	4.8000	7.0000
	q_e (calculated, (mg/g))	10.2200	7.6100	9.9900
	R^2	0.9945	0.9922	0.9982

the reactive media becomes saturated, reducing the delay factor of AMX, showing that the functionality of the reactive media to delay the propagation of AMX decreases. This explains the increase in the concentration of AMX effluents over time. Additionally, the time it takes for the AMX normalized concentration to reach 1 (the saturated state) at the exit of the column ports was quicker in NB-TMAB/GW than in NB-CTAB/GW and CB/GW. This behavior indicates that NB-CTAB/GW has higher activity in removing AMX than CB/GW and NB-TMAB/GW because it has binding sites having a higher affinity for binding with AMX in comparison with other MB. These results are identical to the results of batch experiments, which showed that the ability of NB-CTAB to remove AMX is higher than that of CB and NB-TMAB.

3.6.3. Influence of flow rate

In this section column experiments were performed for three different flow rates 10, 15 and 20 mL/min, as shown in Fig. 13. As the flow rates rose in this diagram, the normalized concentration levels rose quickly and reached saturation (C/C_o = 1). The reason for this behavior is that the

Table 6
Hydraulic conductivity of the used reactive systems

Designation	Hydraulic conductivity, cm/s		
	M1 (2MB/1GW)	M2 (2MB/2GW)	M3 (2MB/3GW)
NB-CTAB/GW	0.0086	0.0217	0.0346
NB-TMAB/GW	0.0107	0.0249	0.0394
CB/GW	0.0119	0.0277	0.0439
NB	10–10		
MB	0.0002–0.0003		
GW	0.0512		

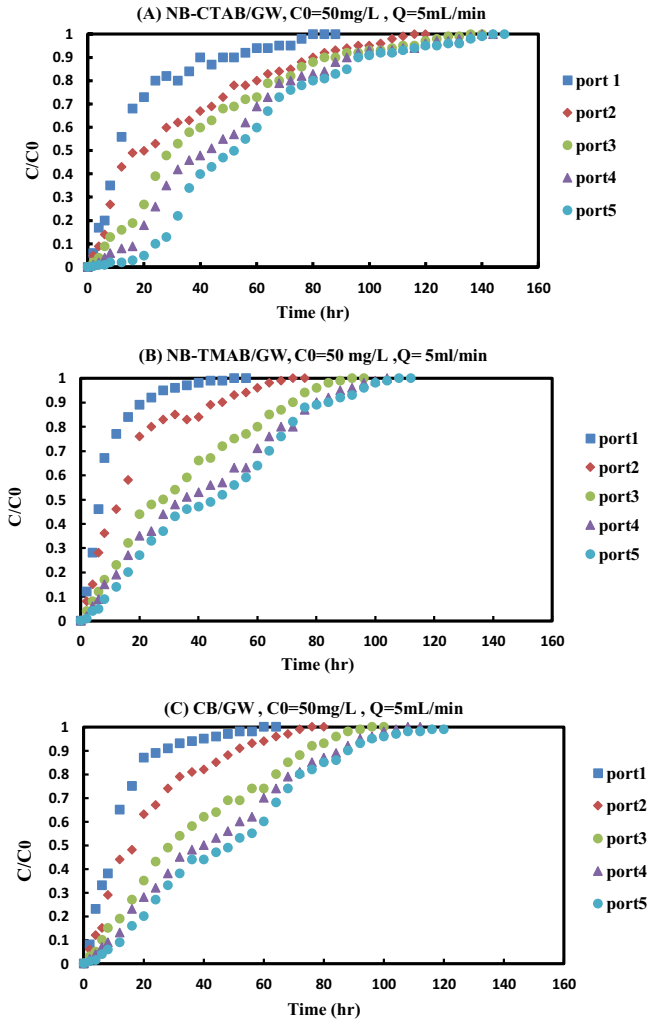

Fig. 12. Breakthrough curves of amoxicillin in the effluent ports of the laboratory column.

contaminant's (AMX) time in the bed column decreased as the flow rate increased, resulting in a shorter stay and a lower removal rate. In addition, due to the potential to degrade the weak ionic bonds between the contaminant and the reactive substance (MB) binding sites, a fast flow rate can also result in a lower removal ratio [45].

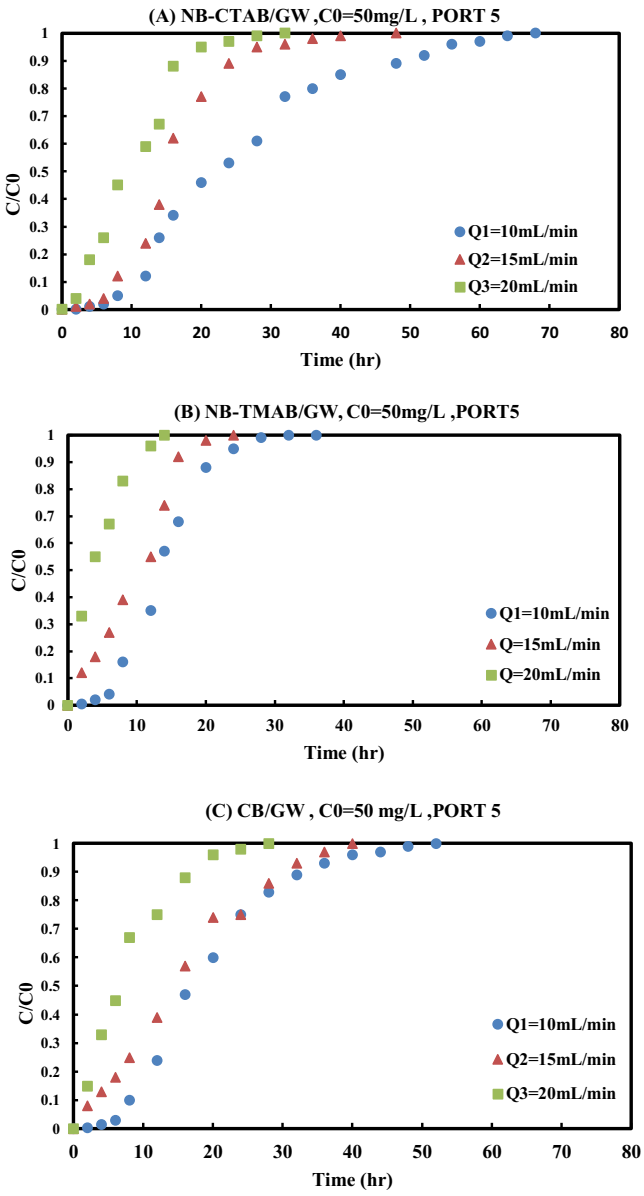

Fig. 13. Breakthrough curves of amoxicillin at different flow rate.

3.6.4. Influence of initial AMX concentration

It is discussed how varying beginning concentrations of AMX 25, 50, and 100 mg/L and a flow rate of 5 mL/min affect the inflow concentration of AMX in the effluent ports in Fig. 14. It can be seen that at higher AMX concentrations, the reactive media begin to saturate, causing the breakthrough curves to begin sloping earlier, indicating a reduction in removal efficiency. Conversely, at lower AMX concentrations, the breakthrough curves take a longer time to rise, indicating the effectiveness of the reactive media, and they remain active for a longer time before they are exhausted [42]. The following is an explanation for this behavior: the low concentration gradient leads to a slow spread of the AMX through the pores due to the reduction in the mass transfer coefficient, which increases the saturation time of the reactive media and vice versa [46]. In addition, the reactive media contains

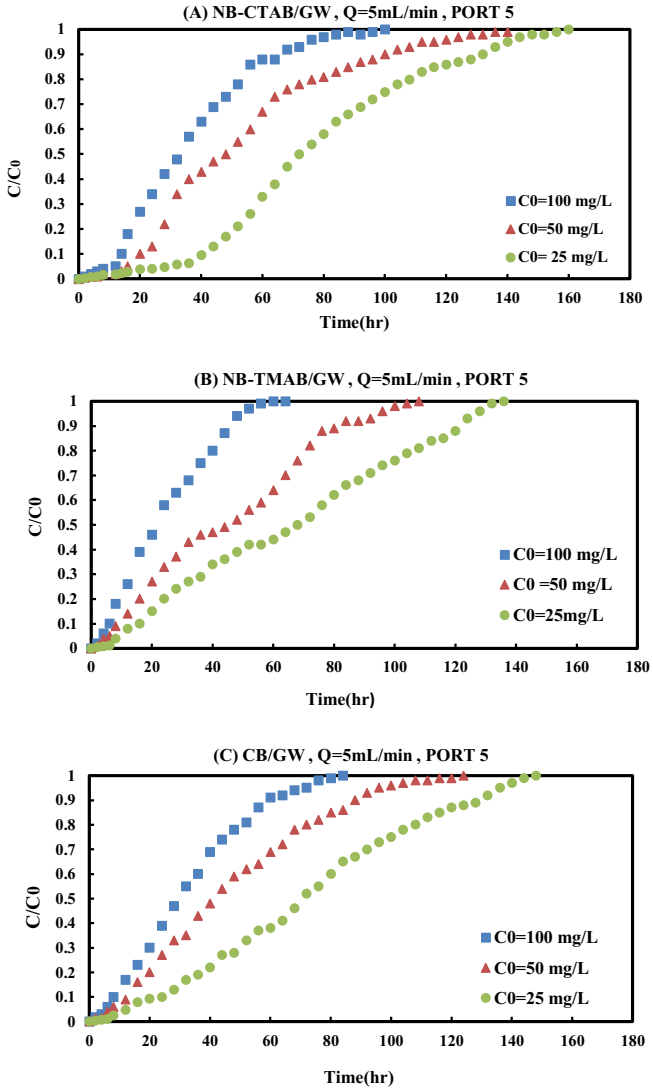

Fig. 14. Breakthrough curves of amoxicillin at different initial concentrations.

a fixed number of active sites, so increasing the initial concentrations of AMX, leads to a decrease in the removal efficiency because the effective sites are already full of AMX and there are no additional active sites available to accommodate an increase in the amount of AMX [47].

3.6.5. Variation of hydraulic conductivity with time

As can be seen from Fig. 15, monitoring variations in the hydraulic conductivity of the column bed at port 5 at specific times was one of the most crucial aspects of the current investigation. The findings were calculated based on Darcy's law, which required knowledge of the entire volume of the treated water. In this experiment, the values of the hydraulic conductivity for the reactive system M2 (2MB/2GW) that are depicted in Table 6 were adopted as initial values of hydraulic conductivity. From Fig. 15 it can be seen that shortly after operation, the hydraulic conductivity values began to slowly decrease and then stabilize at a certain level.

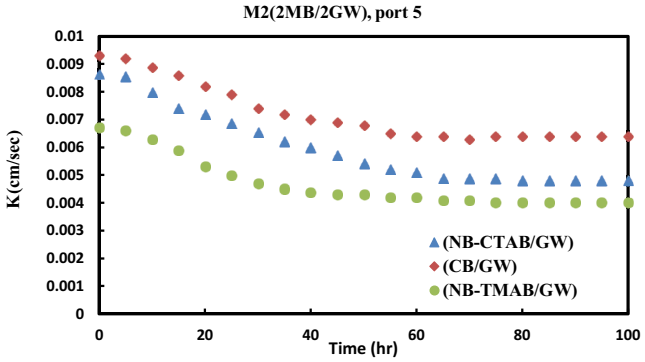

Fig. 15. Variation of hydraulic conductivity as a function of time.

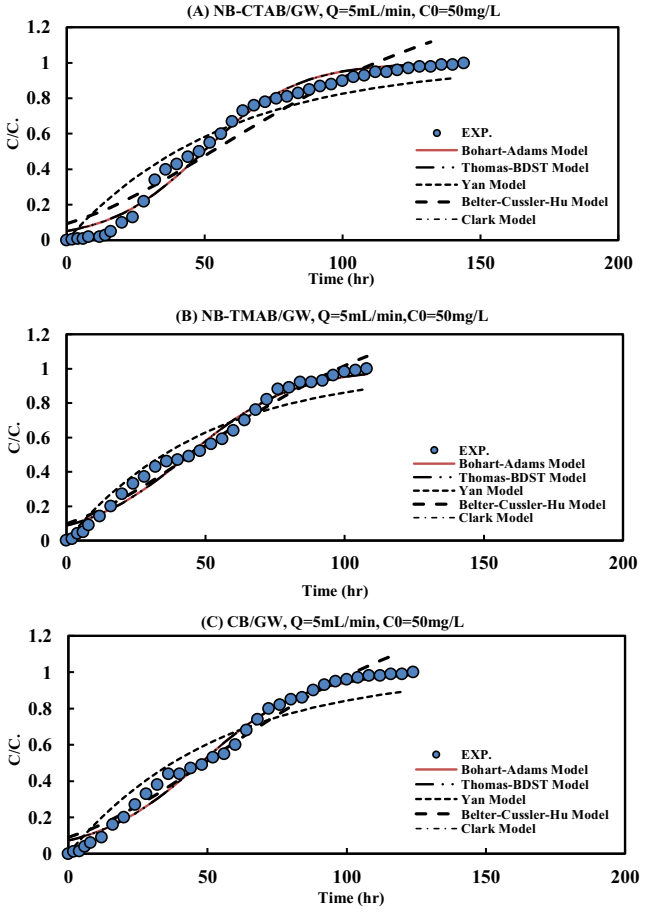

Fig. 16. Variation of amoxicillin normalized concentration sorbed onto column bed (M2) as a function of time (port 5).

In addition, two cases can be observed, the first is that the rate of decrease in the hydraulic conductivity of the reactive medium (NB-CTAB/GW) was more than that of NB-TMAB/GW, and the second is that the rate was the decrease in the hydraulic conductivity of the (CB/GW) is the lowest. For the first case, this is likely related to the rate of AMX accumulation on the surface of the reactive medium, which is directly proportional to the removal ratio. Since the AMX removal of NB-CTAB/GW is higher than that of NB-TMAB/

Table 7
Parameters of breakthrough models with determination coefficients for amoxicillin corresponding to the experimental conditions at port 5

Model name	Parameter	NB-CTAB/GW	NB-TMAB/GW	CB/GW
Bohart–Adams model	k_c	0.05877	0.05336	0.0536
	kN.Z/*u*	2.91681	2.34682	2.5423
	R^2	0.98707	0.98025	0.98696
	SSE	0.0858	0.06977	0.05783
Thomas–BDST model	KTQM/*Q*	2.91681	2.34682	2.5423
	KTC	0.05877	0.05336	0.0536
	R^2	0.98707	0.98025	0.98696
	SSE	0.0858	0.06977	0.05783
Yan model	0.001QC/Q.M	7.4E-05	8.35E-05	7.83E-05
	A	237.679	237.679	237.679
	R^2	0.97407	0.96824	0.96954
	SSE	0.37967	0.17971	0.24396
Belter–Cussler–Hu model	t_0	112.138	97.6451	102.968
	o	0.59517	0.60367	0.58936
	R^2	0.94869	0.9799	0.97893
	SSE	0.28333	0.07235	0.08765
Clark model	*A*	18.3233	10.4523	12.8129
	R	0.05867	0.05336	0.05366
	N	1.99803	2	2.00332
	R^2	0.98632	0.98025	0.98564
	SSE	1.46E-06	1.57E-14	1.9E-07

GW, according to the experimental results, the accumulated amount of AMX of NB-CTAB/GW is greater than that of NB-TMAB/GW. This means that the rate of decrease in the interparticle of the reactive system was greater in the case of NB-CTAB/GW than in the case of NB-TMAB/GW. While in the second case, although CB/GW has a lower AMX removal ratio than NB-CTAB/GW, it has a lower hydraulic conductivity rate decreasing than all due to its exposure to thermal processes that improved its mechanical properties and stability.

3.6.6. Breakthrough curve models

Five models were used to fit experimental measurements from column studies for the elimination of AMX. Bohart–Adams, Thomas–BDST, Yan, Belter–Cussler–Hu, and Clark are some of these models, as shown in Fig. 16. The breakthrough curves of AMX at port 5 for three different types of reactive media are represented by these models in accordance with the experimental parameters used in this section (Q = 5 mL/min, C_o = 50 mg/L). Additionally, statistical measurements like R^2 and sum of squares error were used to show the degree of agreement between the anticipated and experimental results (SSE). According to the following equation, the sum square error was calculated:

$$\mathrm{SSE} = \sum \left[\left(\frac{C}{C_o} \right)_{\text{experimental}} - \left(\frac{C}{C_o} \right)_{\text{predicted}} \right]^2 \tag{19}$$

The parameters of breakthrough models with determination coefficients were estimated by Microsoft Excel 2016. All values of the model parameters, R^2 and SSE for the predicted and experimental results are presented in Table 7. It's clear from this table that the Clark model in comparison to other models is a more accurate representation of the experimental data since it has a lower SSE value for AMX adsorbed in various beds.

4. Conclusion

Based on the results of the batch and continuous experiments, the following conclusions can be drawn:

This study involved the modification of Iraqi natural bentonite (NB) using two cationic surfactants (CTAB and TMAB) with a thermal process as another approach for modification to produce three types of modified bentonite named NB-CTAB, NB-TMAB, and CB, they were used as reactive materials for removal of AMX from aqueous solutions using batch and continuous modes.

The optimal ratio of (CTAB and TMAB)/NB that resulted in the highest AMX removal percent was 0.5 g·CTAB/g·NB and 0.6 g·TMAB/g·NB that increased the efficiency of the natural bentonite to about 6.5 and 4 times.

The parameters studied in batch mode such as contact time, initial solution pH, agitation speed, initial AMX concentration and MB dosage were factors influencing the AMX removal process. The best values for these parameters were 3.5 h, 10, 6, 10 and 250 rpm, 50 mg/L, 0.7, 0.9, and

0.8 g/100 mL which provide maximum removal efficiencies of 96%, 70% and 94% for NB-CTAB, NB-TMAB, and CB, respectively.

The experimental findings shown that the Freundlich isotherm model can accurately explain the sorption data for MB (NB-CTAB, NB-TMAB, and CB) with an R^2 of not less than 0.9123.

The findings of the sorption kinetics demonstrate that the experimental data were more accurately modeled by the pseudo-second-order model, which demonstrated that chemisorption was the dominating process.

The reactive system M2 (2MB/2GW) was more appropriate than other systems used as a reactive media in continuous mode, so it adopted in all column experiments.

The results of continuous experiments showed the AMX spread was restricted by the reactive media in different proportions, the AMX spread in bed (NB-TMAB/GW) was faster than the two other reactive beds at the same flow rate and run time.

Five breakthrough curve models were used to fit the continuous experimental data: Clark, Yan, Thomas, Bohart–Adams, and Belter–Cussler–Hu models. Comparing the Clark model to other models, it was the one that best captured the experimental findings.

References

[1] V. Homem, L. Santos, Degradation and removal methods of antibiotics from aqueous matrices—a review, J. Environ. Manage., 92 (2011) 2304–2347.

[2] E.K. Putra, R. Pranowo, J. Sunarso, N. Indraswati, S. Ismadji, Performance of activated carbon and bentonite for adsorption of amoxicillin from wastewater: mechanisms, isotherms and kinetics, Water Res., 43 (2009) 2419–2430.

[3] B.H. Graimed, Z.T. Abd Ali, Thermodynamic and kinetic study of the adsorption of Pb(II) from aqueous solution using bentonite and activated carbon, Al-Khwarizmi Eng. J., 9 (2013) 48–56.

[4] A.A. Faisal, Z.T. Abd Ali, Groundwater protection from lead contamination using granular dead anaerobic sludge biosorbent as permeable reactive barrier, Desal. Water Treat., 57 (2016) 3891–3903.

[5] A.F. de Almeida Neto, M.G.A. Vieira, M.G.C. da Silva, Cu(II) adsorption on modified bentonitic clays: different isotherm behaviors in static and dynamic systems, Mater. Res., 15 (2012) 114–124.

[6] R. Guégan, Intercalation of a nonionic surfactant (C10E3) bilayer into a Na-montmorillonite clay, Langmuir, 26 (2010) 19175–19180.

[7] R. Guegan, Self-assembly of a non-ionic surfactant onto a clay mineral for the preparation of hybrid layered materials, Soft Matter, 9 (2013) 10913–10920.

[8] R. Guegan, T. De Oliveira, J. Le Gleuher, Y. Sugahara, Tuning down the environmental interests of organoclays for emerging pollutants: pharmaceuticals in presence of electrolytes, Chemosphere, 239 (2020) 124730, doi: 10.1016/j.chemosphere.2019.124730.

[9] H. He, Y. Ma, J. Zhu, P. Yuan, Y. Qing, Organoclays prepared from montmorillonites with different cation exchange capacity and surfactant configuration, Appl. Clay Sci., 48 (2010) 67–72.

[10] S.M. Ibrahim, Z.T.A. Ali, Removal of acidic dye from aqueous solution using surfactant modified bentonite (organoclay): batch and kinetic study, J. Eng., 26 (2020) 64–81.

[11] M.F. Oliveira, M.G.C. da Silva, M.G.A. Vieira, Equilibrium and kinetic studies of caffeine adsorption from aqueous solutions on thermally modified Verde-lodo bentonite, Appl. Clay Sci., 168 (2019) 366–373.

[12] M. Toor, B. Jin, S. Dai, V. Vimonses, Activating natural bentonite as a cost-effective adsorbent for removal of Congo-red in wastewater, J. Ind. Eng. Chem., 21 (2015) 653–661.

[13] M.A. Osman, M. Ploetze, P. Skrabal, Structure and properties of alkyl ammonium monolayers self-assembled on montmorillonite platelets, J. Phys. Chem., B, 108 (2004) 2580–2588.

[14] Maged, J. Iqbal, Sh. Kharbish, I.S. Ismael, A. Bhatnagar, Tuning tetracycline removal from aqueous solution onto activated 2:1 layered clay mineral: characterization, sorption and mechanistic studies, J. Hazard. Mater., 384 (2020) 121320, doi: 10.1016/j.jhazmat.2019.121320.

[15] Z.T.A. Ali, Green synthesis of graphene-coated sand (GCS) using low-grade dates for evaluation and modeling of the pH-dependent permeable barrier for remediation of groundwater contaminated with copper, Sep. Sci. Technol., 56 (2021) 14–25.

[16] Z.T.A. Ali, H.J. Khadim, M.A. Ibrahim, Simulation of the remediation of groundwater contaminated with ciprofloxacin using grafted concrete demolition wastes by ATPES as reactive material: batch and modeling study, Egypt. J. Chem., 65 (2022) 585–596.

[17] A.A.H. Faisal, Z.T.A. Ali, Using sewage sludge as a permeable reactive barrier for remediation of groundwater contaminated with lead and phenol, Sep. Sci. Technol., 52 (2017) 732–742.

[18] A.F. Ali, Z.T.A. Ali, Interaction of aqueous Cu^{2+} ions with granules of crushed concrete, Iraqi J. Chem. Petrol. Eng., 20 (2019) 31–38.

[19] A.F. Ali, Z.T.A. Ali, Sustainable use of concrete demolition waste as reactive material in permeable barrier for remediation of groundwater: batch and continuous study, J. Environ. Eng., 146 (2020) 04020048, doi: 10.1061/(ASCE)EE.1943-7870.0001714.

[20] Z.T. Abd Ali, A comparative isothermal and kinetic study of the adsorption of lead(II) from solution by activated carbon and bentonite, J. Eng., 21 (2015) 45–58.

[21] N. Saad, Z.T. Abd Ali, L.A. Naji, A.A. Faisal, N. Al-Ansari, Development of Bi-Langmuir model on the sorption of cadmium onto waste foundry sand: effects of initial pH and temperature, Environ. Eng. Res., 25 (2020) 677–684.

[22] Z.T. Abd Ali, L.A. Naji, S.A. Almuktar, A.A.H. Faisal, S.N. Abed, M. Scholz, M. Naushad, T. Ahamad, Predominant mechanisms for the removal of nickel metal ion from aqueous solution using cement kiln dust, J. Water Process Eng., 33 (2020) 101033, doi: 10.1016/j.jwpe.2019.101033.

[23] A.A.H. Faisal, Z.T.A. Ali, Remediation of groundwater contaminated with the lead–phenol binary system by granular dead anaerobic sludge-permeable reactive barrier, Environ. Technol., 38 (2017) 2534–2542.

[24] A.A.H. Faisal, Z.T.A. Ali, Phenol removal using granular dead anaerobic sludge permeable reactive barrier in a simulated groundwater pilot plant, J. Eng., 20 (2014) 63–79.

[25] Z.T.A. Ali, Green synthesis of graphene-coated glass as novel reactive material for remediation of fluoride-contaminated groundwater, Desal. Water Treat., 226 (2021) 113–124.

[26] B.H. Graimed, Z.T. Abd Ali, Batch and continuous study of one-step sustainable green graphene sand hybrid synthesized from date-syrup for remediation of contaminated groundwater, Alexandria Eng. J., 61 (2022) 8777–8796.

[27] B.H. Graimed, Z.T.A. Ali, Green approach for the synthesis of graphene glass hybrid as a reactive barrier for remediation of groundwater contaminated with lead and tetracycline, Environ. Nanotechnol. Monit. Manage., 18 (2022) 100685, doi: 10.1016/j.enmm.2022.100685.

[28] A.H. Sulaymon, A.A.H. Faisal, Z.T.A. Ali, Performance of granular dead anaerobic sludge as permeable reactive barrier for containment of lead from contaminated groundwater, Desal. Water Treat., 56 (2015) 327–337.

[29] P.-X. Lee, B.-L. Liu, P.L. Show, C.W. Ooi, W.S. Chai, H.S.H. Munawaroh, Y.-K. Chang, Removal of calcium ions from aqueous solution by bovine serum albumin (BSA)-modified nanofiber membrane: dynamic adsorption performance and

breakthrough analysis, Biochem. Eng. J., 171 (2021) 108016, doi: 10.1016/j.bej.2021.108016.
[30] Z.T. Abd Ali, Z.Z. Ismail, Experimental and modeling study of water defluoridation using waste granular brick in a continuous up-flow fixed bed, Environ. Eng. Res., 26 (2021) 190506, doi: 10.4491/eer.2019.506.
[31] M.L. Cantuaria, E.S. Nascimento, A.F.A. Neto, O.A.A. dos Santos, M.G.A. Vieira, Removal and recovery of silver by dynamic adsorption on bentonite clay using a fixed-bed column system, Adsorpt. Sci. Technol., 33 (2015) 91–103.
[32] C.-G. Lee, J. Kim, J.-H. Kim, J.-K. Kang, S.-B. Kim, S.-J. Park, S.-H. Lee, J.-W. Choi, Comparative analysis of fixed-bed sorption models using phosphate breakthrough curves in slag filter media, Desal. Water Treat., 55 (2015) 1795–1805.
[33] G.S. Bohart, E.Q. Adams, Some aspects of the behavior of charcoal with respect to chlorine, J. Am. Chem. Soc., 42 (1920) 523–544.
[34] Z.T.A. Ali, Combination of the artificial neural network and advection-dispersion equation for modeling of methylene blue dye removal from aqueous solution using olive stones as reactive bed, Desal. Water Treat., 179 (2020) 302–311.
[35] Z. Huang, Y. Li, W. Chen, J. Shi, N. Zhang, X. Wang, Z. Li, L. Gao, Y. Zhang, Modified bentonite adsorption of organic pollutants of dye wastewater, Mater. Chem. Phys., 202 (2017) 266–276.
[36] T. De Oliveira, R. Guégan, T. Thiebault, C.L. Milbeau, F. Muller, V. Teixeira, M. Giovanela, M. Boussafir, Adsorption of diclofenac onto organoclays: effects of surfactant and environmental (pH and temperature) conditions, J. Hazard. Mater., 323 (2017) 558–566.
[37] D.L. Pavia, G.M. Lampman, G.S. Kriz, J.R. Vyvyan, Introduction to Spectroscopy, 4th ed., Brooks/Cole, Belmont, CA, 2010.
[38] K.H. Chu, Improved fixed bed models for metal biosorption, Chem. Eng. J., 97 (2004) 233–239.
[39] Y. Wan, D. Guo, X. Hui, L. Liu, Y. Yao, Studies on hydration swelling and bound water type of sodium- and polymer-modified calcium bentonite, Adv. Polym. Technol., 2020 (2020) 1–11.
[40] A.H. Sulaymon, Z.T. Abd Ali, Removal of kerosene from wastewater using Iraqi bentonite, J. Eng., 16 (2010) 5422–5437.
[41] Z. Alakayleh, T.P. Clement, X. Fang, Understanding the changes in hydraulic conductivity values of coarse- and fine-grained porous media mixtures, Water, 10 (2018) 313, doi: 10.3390/w10030313.
[42] Z.T. Abd Ali, H.M. Flayeh, M.A. Ibrahim, Numerical modeling of performance of olive seeds as permeable reactive barrier for containment of copper from contaminated groundwater, Desal. Water Treat., 139 (2019) 268–276.
[43] L.A. Naji, S.H. Jassam, M.J. Yaseen, A.A.H. Faisal, N. Al-Ansari, Modification of Langmuir model for simulating initial pH and temperature effects on sorption process, Sep. Sci. Technol., 55 (2020) 2729–2736.
[44] M.N. Ezzat, Z.T.A. Ali, Green approach for fabrication of graphene from polyethylene terephthalate (PET) bottle waste as reactive material for dyes removal from aqueous solution: batch and continuous study, Sustainable Mater. Technol., 32 (2022) e00404, doi: 10.1016/j.susmat.2022.e00404.
[45] Z.B. Masood, Z.T.A. Ali, Numerical modeling of two-dimensional simulation of groundwater protection from lead using different sorbents in permeable barriers, Environ. Eng. Res., 25 (2020) 605–613.
[46] T.H. Mhawesh, Z.T.A. Ali, Reuse of brick waste as a cheap-sorbent for the removal of nickel ions from aqueous solutions, Iraqi J. Chem. Petrol. Eng., 21 (2020) 15–23.
[47] A.A.H. Faisal, Z.T.A. Ali, Using granular dead anaerobic sludge as permeable reactive barrier for remediation of groundwater contaminated with phenol, J. Environ. Eng., 141 (2015) 04014072, doi: 10.1061/(ASCE)EE.1943-7870.0000903.
[48] M.M. Abu-Zreig, N.M. Al-Akhras, M.F. Attom, Influence of heat treatment on the behavior of clayey soils, Appl. Clay Sci., 20 (2001) 129–135.
[49] S. Ghaderi, F. Moeinpour, F.S. Mohseni-Shahri, Removal of Zn(II) from aqueous solutions using $NiFe_2O_4$ coated sand as an efficient and low cost adsorbent: adsorption isotherm, kinetic and thermodynamic studies, Phys. Chem. Res., 6 (2018) 839–855.
[50] A.G. Espantaleón, J.A. Nieto, M. Fernández, A. Marsal, Use of activated clays in the removal of dyes and surfactants from tannery waste waters, App. Clay Sci., 24 (2003) 105–110.
[51] Sh.X. Zha, Y. Zhou, X. Jin, Z. Chen, The removal of amoxicillin from wastewater using organobentonite, J. Environ. Manage., 129 (2013) 569–576.
[52] H. Han, M.K. Rafiq, T. Zhou, R. Xu, O. Mašek, X. Li, A critical review of clay-based composites with enhanced adsorption performance for metal and organic pollutants, J. Hazard. Mater., 369 (2019) 780–796.
[53] H. Gallouze, D.-E. Akretche, C. Daniel, I. Coelhoso, J.G. Crespo, Removal of synthetic estrogen from water by adsorption on modified bentonites, Environ. Eng. Sci., 38 (2020) 4–14.